Brazilian Journal of Physics
ISSN: 0103-9733
luizno.bjp@gmail.com
Sociedade Brasileira de Física
Brasil

Venkateswarlu, C.; Ratnakaram, Y. C.; Seshadri, M.; Thirupathi Naidu, D.
Spectral Investigations on Ho3+ Doped Mixed Alkali Chloroborate Glasses
Brazilian Journal of Physics, vol. 41, núm. 4-6, 2011, pp. 281-289
Sociedade Brasileira de Física
Sâo Paulo, Brasil

Braz J Phys (2011) 41:281–289
DOI 10.1007/s13538-011-0047-9

GENERAL AND APPLIED PHYSICS

Spectral Investigations on Ho^{3+} Doped Mixed Alkali Chloroborate Glasses

C. Venkateswarlu · Y. C. Ratnakaram · M. Seshadri · D. Thirupathi Naidu

Received: 10 May 2011 / Published online: 5 October 2011

Abstract The optical absorption and emission spectra of two different Ho^{3+} doped mixed alkali chloroborate glasses have been studied in the ultraviolet-visible near-infrared regions. Various spectroscopic parameters like Racah (E^1, E^2, and E^3), spin orbit (ξ_{4f}), and configuration interaction (α) parameters have been calculated. From the measured spectral intensities of the various absorption bands of Ho^{3+} ion, the Judd–Ofelt intensity parameters (Ω_2, Ω_4, and Ω_6) have been evaluated and covalency was studied as a function of x in the glass matrices. Using these parameters, radiative transition probabilities, radiative lifetimes, branching ratios, and integrated absorption cross-sections have been calculated and reported for certain excited states of Ho^{3+} ion. From the emission spectra, stimulated emission cross-sections are determined for the emission transitions, $^5F_4$, $^5S_2 \rightarrow {}^5I_8$, and $^5F_5 \rightarrow {}^5I_8$ in these two mixed alkali chloroborate glasses. An attempt has been made to throw some light on the environment of Ho^{3+} ions in these glass systems by studying the variation in various spectroscopic parameters.

Keywords Borate glass · Absorption · Emission · Judd–Ofelt theory · Cross-section · Rare earth ion

1 Introduction

The electronic energy levels of the rare earth ions determine the lasing characteristics of rare-earth doped materials and are influenced considerably by the presence of other ions in their vicinity [1–3]. The radiative properties of rare earth ions doped in host matrices are different from that of a free ion due to local perturbations and due to electric fields of the host ions. A lot of interest was focused on glasses and optical fibers for their utility as the laser emitting at 2 μm. The optical fiber lasers operating at 2.1 μm have been reported with Ho- and Yb/Ho-doped fibers [4, 5]. Hence, Ho^{3+}-doped glasses are gaining popularity as they have many capabilities such as 2 μm emission, visible wavelength upconversion, and emission in the 800 nm band. Ho^{3+} ions can produce laser emission in 2.0 and 2.9 μm ranges arising from the transitions, $^5I_7 \rightarrow {}^5I_8$ and $^5I_6 \rightarrow {}^5I_8$, respectively [6–8]. Ho^{3+} ion has several low-lying metastable levels, which can give rise to transitions at various wavelengths from infrared to ultraviolet regions. Recently, considerable amount of research work has been done on absorption and emission properties of Ho^{3+} in various glass materials [9–13].

Mixed alkali effect is one of the problems in glass science that has been subjected to study for some decades. In a mixed alkali borate glass, if one alkali oxide is progressively substituted by another, some of the properties like resistivity do not vary linearly but goes through a maximum when the two alkalies are present in approximately equal concentration. This is commonly known as mixed alkali effect [14]. With the addition of alkali oxides, the structural variations that take place in B_2O_3 are quite different compared to silicates. In borate glasses, conversion of BO_3 units to tetrahedral BO_4 units takes place without the creation of nonbridging oxygens. From the X-ray diffraction study of a series of alkali borate glasses, Bisco et al. [15] have first observed the evidence for this change in the boron coordination. For alkali borate glasses, the abrupt property changes were observed nearly at 15–20 mol% modifier oxide [16]. This peculiar and anomalous behavior, referred to as "borate anomaly" was first

C. Venkateswarlu · Y. C. Ratnakaram (✉) · M. Seshadri
Department of Physics, Sri Venkateswara University,
Tirupati 517-501, AP, India
e-mail: ratnakaram_yc@yahoo.co.in

D. T. Naidu
Department of Physics, Rao & Naidu Engineering College,
Ongole 523001, AP, India

explained in terms of the unique ability of boron to exist in two distinct coordination states, the trigonal and tetrahedral. The addition of alkali oxide to boric oxide results in conversion of boron from trigonal to tetrahedral coordination up to 20 and at 20 mol% of R_2O (R=Li, Na, K, and Rb) the tetraborate reaches maximum concentration, the boroxyl group disappears and the formation of diborate starts. In the present work, the authors report the optical properties of Ho^{3+} ions doped two different mixed alkali chloroborate glasses keeping in mind the mixed alkali effect and "borate anomaly" [16]. Various spectroscopic parameters like Racah (E^1, E^2, and E^3), spin orbit (ξ_{4f}), and configuration interaction (α) parameters are deduced as a function of alkali content in the glass matrix. Using Judd–Ofelt theory, radiative and nonradiative properties are studied and some of the potential lasing transitions are identified. From the emission spectra, emission cross-sections are calculated and their variation with the variation of alkali content in the two glass matrices has been studied.

2 Experimental Details

The glasses were prepared using conventional melt-quenching method. High purity reagent chemicals H_3BO_3, LiCl, NaCl, KCl, and Ho_2O_3 were used as the starting materials. The compositions studied in the present work are $69.5H_3BO_3$–xLiCl–(30-x)NaCl–$0.5Ho_2O_3$ and $69.5H_3BO_3$–xLiCl–(30-x)KCl–$0.5Ho_2O_3$ (where x=5, 10, 15, 20, and 25). The anhydrous chlorides were dried by heating at appropriate temperatures under vacuum. A small amount of ammonium chloride was added to these dehydrated chlorides in order to drive off impurities. Accurately weighed 6–8 g batches were thoroughly ground using agate mortar and heated in a silica crucible for 2 h in an electric furnace at a temperature of 400°C. This allowed the phosphorus pentoxide to decompose and react with other batch constituents before melting. The batches were melted in a silica crucible at 900°C in an electric furnace in air atmosphere. The melt was cast onto a preheated brass mold at 400°C to prevent the fast cooling. To reduce the internal strain, the glasses were annealed with a thermal treatment at 300°C for 2 h. For convenience, these glass systems are designated as lithium–sodium chloroborate glass (LSCBG) for $69.5H_3BO_3$–xLiCl–(30-x)NaCl–$0.5Ho_2O_3$ and lithium–potassium chloroborate glass (LPCBG) for $69.5H_3BO_3$–xLiCl–(30-x)KCl–$0.5Ho_2O_3$ glass compositions. The densities of the glass samples were measured using an Archimedes principle. The refractive indices were determined with an Abbe refractometer using monobromonaphthalene as adhesive coating with an accuracy of ±0.001 and the sample thicknesses were obtained using a micrometer. The optical absorption spectra were recorded in the wavelength region 350–950 nm, using JASCO V-570 spectrometer and emission spectra were measured in the wavelength region of 550–700 nm using Fluoro Max-3 Photoluminescence Spectrometer.

3 Results and Discussion

Spectroscopic Parameters

Optical absorption spectra of Ho^{3+} doped lithium–sodium mixed alkali chloroborate glass for different x values in the glass matrix in the wavelength range 350–950 nm are shown in Fig. 1. The absorption spectra of Ho^{3+} in lithium–potassium mixed alkali chloroborate glasses are not shown as they are similar in shape. The transitions were assigned by comparing the band positions in the absorption spectrum with an energy level scheme of LaF_3/Ho^{3+} published by Carnall et al. [17]. The experimental energies of all the observed bands of Ho^{3+} ion in the two glass matrices are presented in Table 1. Racah (E^1, E^2, and E^3), spin orbit (ξ_{4f}), and configuration interaction (α) parameters are obtained for all the glass matrices using the procedure explained in [18]. The calculated energy values are also obtained. These values are presented in Table 1 along with the root-mean-square (rms) deviations between experimental and calculated energies. The rms deviation values are very small indicating that a full matrix diagonalization procedure leads to a good fit between the experimental and calculated energies. The hydrogenic ratios (E^1/E^3 and E^2/E^3) which indicate radial properties are more or less same for all the mixed alkali borate glasses indicating that these properties are not much affected with the variation of alkali contents in the glass matrices.

3.1 Spectral Intensities and Judd–Ofelt Parameters

The spectral intensities of the observed bands (experimental (f_{exp})) were determined by measuring the areas under the absorption curves using the relation [17]

$$f_{exp} = 4.32 \times 10^{-9} \int \varepsilon(\nu) d\nu \quad (1)$$

where, $\varepsilon(\nu)$ is the molar absorptivity of a band at mean energy ν per centimeter and may be computed from the measured absorbance "A" for known concentrations of the Ho^{3+} ions and the thickness of the sample. The theoretical oscillator strengths (calculated (f_{cal})) of the electric dipole transitions within f^N configurations were calculated using standard Judd–Ofelt theory [19, 20]

$$f_{cal}(aJ, bJ') = \frac{8\pi^2 mc}{3h(2J+1)} \frac{1}{\lambda} \frac{(n^2+2)^2}{9n} \times \sum_{\lambda=2,4,6} \Omega_\lambda \|\langle (SL)J \rangle \| U^\lambda \| (S'L')J' \|^2 \quad (2)$$

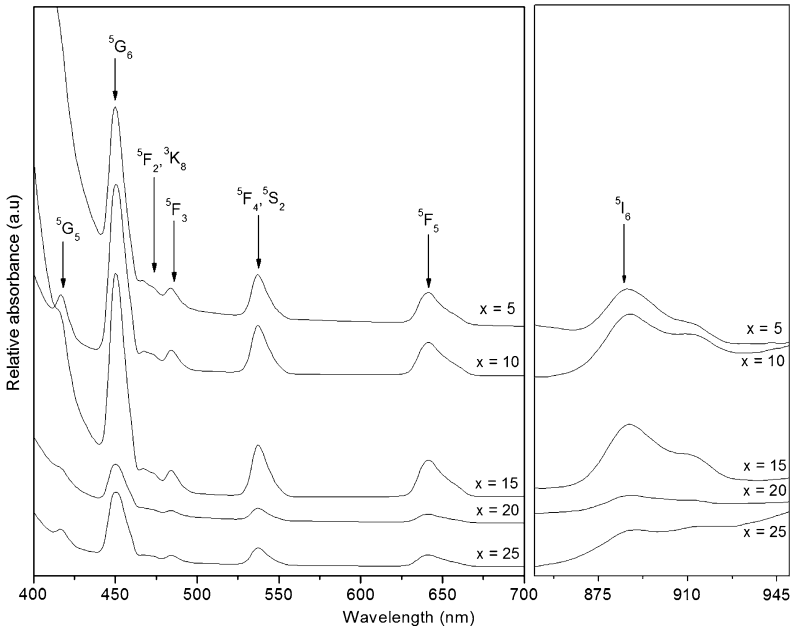

Fig. 1 Optical absorption spectra of Ho^{3+} doped lithium–sodium mixed alkali chloroborate glasses (all the transitions shown are from the ground state $^5|_8$). Figure shows decreasing intensity of $^5|_8 \rightarrow {}^5|_8$ transition with increasing lithium content (x) in the glass matrix

where Ω_λ are Judd–Ofelt intensity parameters and $\left\|U^\lambda\right\|^2$ are the squared reduced matrix elements of the unit tensor operator of rank λ=2, 4, and 6, which were taken from literature [19]. The remaining symbols have their usual meanings. Experimental (f_{exp}) and calculated (f_{cal}) spectral intensities of the observed absorption bands in lithium–sodium and lithium–potassium mixed alkali chloroborate glasses obtained in the present work are presented in Table 2. It is observed that the spectral intensities of most of the absorption bands are higher at x=10−15 mol% and lower at x=20–25 mol% in both lithium–sodium and lithium–potassium glass matrices indicating that nonsymmetric component of crystal field acting on Ho^{3+} ions is stronger and weaker at these compositions respectively. The small rms deviations between the experimental and calculated spectral intensities confirm the validity of approximations made in Judd–Ofelt theory. Substituting f_{exp} for f_{cal} and using the least-square fit method, the three intensity parameters, Ω_λ (λ=2, 4, and 6) are obtained. The resulting best set of Judd–Ofelt parameters is presented in Table 3 for both lithium–sodium and

Table 1 Experimental energies (E_{exp}; cm^{-1}) and various spectroscopic parameters (E^1, E^2, E^3, ξ_{4f}, and α) of Ho^{3+} doped mixed alkali chloroborate glasses (x in mol%)

S. no	Energy level	Lithium–sodium glass					Lithium–potassium glass				
		x=5	x=10	x=15	x=20	x=25	x=5	x=10	x=15	x=20	x=25
1	$^5I_5$	11,279	11,274	11,274	11,274	11,258	11,258	11,280	11,280	11,291	11,293
2	$^5F_5$	15,591	15,603	15,581	15,586	15,591	15,574	15,595	15,622	15,613	15,598
3	$^5F_4$, $^5S_2$	18,622	18,611	18,608	18,629	18,622	18,601	18,629	18,622	18,622	18,622
4	$^5F_3$	20,674	20,640	20,652	20,652	20,678	20,644	20,644	20,678	20,644	20,695
5	$^5F_2$, $^3K_8$	21,445	21,404	21,404	21,417	21,376	21,454	21,367	21,408	21,418	21,381
6	$^5G_6$	22,232	22,197	22,212	22,232	22,237	22,281	22,202	22,232	22,192	22,187
7	$^5G_5$	–	23,969	24,061	24,015	24,038	–	24,003	24,079	23,992	24,056
	Rms Deviation	±37	±22	±30	±45	±17	±01	±24	±04	±23	±01
	E^1	6,871	6,982	6,903	6,916	6,827	7,875	6,977	6,945	7,029	6,862
	E^2	29.7	31.2	30.3	30.6	30.4	32.8	31.9	30.9	31.5	30.6
	E^3	611	606	611	610	615	663	609	611	605	613
	ξ_{4f}	2,163	2,159	2,162	2,162	2,162	2,165	2,162	2,162	2,162	2,168
	α	13.5	13.7	15.4	14.0	15.8	103.5	16.1	15.8	14.2	17.10
	E^1/E^2	11.2	11.5	11.3	11.3	11.1	11.8	11.4	11.3	11.6	11.2
	E^2/E^3	0.05	0.05	0.05	0.05	0.05	0.05	0.05	0.05	0.05	0.05

Table 2 Experimental spectral intensities ($f_{exp}\times10^6$) of Ho^{3+} doped mixed alkali chloroborate glasses (x in mol%)

S. no	Energy level	Lithium–sodium glass					Lithium–potassium glass				
		x=5	x=10	x=15	x=20	x=25	x=5	x=10	x=15	x=20	x=25
1	$^5I_5$	0.24	0.34	0.38	0.08	0.11	0.19	0.27	0.32	0.20	0.15
2	$^5F_5$	5.61	6.93	6.64	1.65	2.56	4.44	5.60	5.98	4.31	3.11
3	$^5F_4$, $^5S_2$	6.81	8.54	8.39	2.17	3.32	5.26	7.87	7.53	5.53	4.03
4	$^5F_3$	1.30	1.91	1.95	0.43	0.72	0.79	1.65	1.56	1.14	0.79
5	$^5F_2$,$^3K_8$	0.78	0.64	1.12	0.11	0.26	0.43	0.65	0.61	0.36	0.29
6	$^5G_6$	30.07	40.35	40.03	9.55	16.43	26.09	35.71	32.37	24.63	16.01
7	$^5G_5$	–	7.24	4.58	0.83	1.60	–	4.84	4.18	3.32	1.74
	rms Deviation	±0.88	±1.31	±1.35	±0.45	±0.62	±0.77	±1.27	±1.34	±1.12	±0.77

lithium–potassium mixed alkali chloroborate glass matrices. In the present work, the Ω_2 parameter is higher at x=15 mol% and lower at x=20 mol% in lithium–sodium chloroborate glass and in lithium–potassium chloroborate glass; it is higher at x=10 mol% and lower at x=25 mol% indicating higher and lower covalencies of Ho–O bond in these two glass matrices, respectively. The Ω_6 parameter is also higher at x=15 mol% and lower at x=20 mol% in lithium–sodium glass, but it is minimum at x=5 mol% and maximum at x=15 mol% in lithium–potassium glass indicating lower and higher rigidities of the glass matrices at these compositions in the two glass matrices. The values of Judd–Ofelt parameters are also useful in calculating the spectroscopic quality factor $\chi=\Omega_4/\Omega_6$, which is critically important in predicting the stimulated emission for the laser active medium. These values are also presented in Table 3. The spectroscopic quality factor χ is higher at x=5 mol% and lower at x=20 mol% in both the glass matrices. It is observed that in the present work, the spectroscopic quality factor is decreasing with the increase of lithium content in both the glass matrices. Judd–Ofelt intensity parameters, Ω_λ can also be written as [21]

$$\Omega_\lambda = (2t+1)\sum_{s,p}\left|A_{s,p}\right|^2\Xi^2(s,t)(2s+1)^{-1}, \lambda = 2,4,6 \qquad (3)$$

where $A_{s,p}$ are the components of the crystal field operators of rank s and are related to the symmetry of the crystal field around Ho^{3+} ions. Ξ is related to matrix elements between the two radial wave functions of 4f and the admixing levels, e.g., 5d, 5g, and the energy difference between these levels. It has been suggested by Reisfeld [22] that Ξ correlates to the nephelauxetic parameter, β which indicates the degree of covalency of Ho–O bond. Variation of Judd–Ofelt intensity parameters (Ω_2 and $\Sigma\Omega_\lambda$) with the variation of x in lithium–sodium and lithium–potassium glass matrices is shown in Fig. 2.

Table 3 Judd–Ofelt intensity parameters ($\Omega_\lambda\times10^{20}$; cm^2) of Ho^{3+} doped mixed alkali chloroborate glasses (x in mol%)

S. no	Glass matrix	Ω_2	Ω_4	Ω_6	$x=\Omega_4/\Omega_6$
	LSCBG				
1	x=5	5.66	6.71	2.01	3.34
2	x=10	9.02	6.59	3.05	2.16
3	x=15	9.87	5.49	3.91	1.40
4	x=20	2.40	0.98	0.97	1.01
5	x=25	4.16	1.67	1.48	1.23
	LPCBG				
6	x=5	5.01	5.68	1.36	4.18
7	x=10	8.56	4.54	3.11	1.46
8	x=15	7.63	4.28	3.16	1.35
9	x=20	6.01	2.86	2.78	1.02
10	x=25	3.85	1.94	1.77	1.09

3.2 Hypersensitive Transitions

$^5I_8\rightarrow{}^3H_6$ and $^5I_8\rightarrow{}^5G_6$ are the hypersensitive transitions (HST) for Ho^{3+} ion [21]. These transitions will obey the selection rules $\Delta L\leq0$, $\Delta J\leq0$, and $\Delta S=0$ and they are sensitive to the environment. In the present work, the HST, $^5I_8\rightarrow{}^3H_6$ is not observed due to shift in the absorption edge towards shorter wavelength side. The other HST, $^5I_8\rightarrow{}^5G_6$ is observed in all the glass matrices. The peak wavelengths (λ) (nm) and spectral intensities (f) of the HST and Ω_2 (cm^2) parameter in the two glass matrices are given below.

mol%	LSCBG			LPCBG		
	λ	$f\times10^6$	$\Omega_2\times10^{20}$	λ	$f\times10^6$	$\Omega_2\times10^{20}$
x=5	449.8	30.07	5.66	448.8	26.09	5.01
x=10	450.5	40.35	9.02	450.4	35.71	8.56
x=15	450.2	40.03	9.87	449.8	32.37	7.63
x=20	449.8	9.55	2.40	450.6	24.63	6.01
x=25	449.7	16.43	4.16	450.7	16.01	3.85

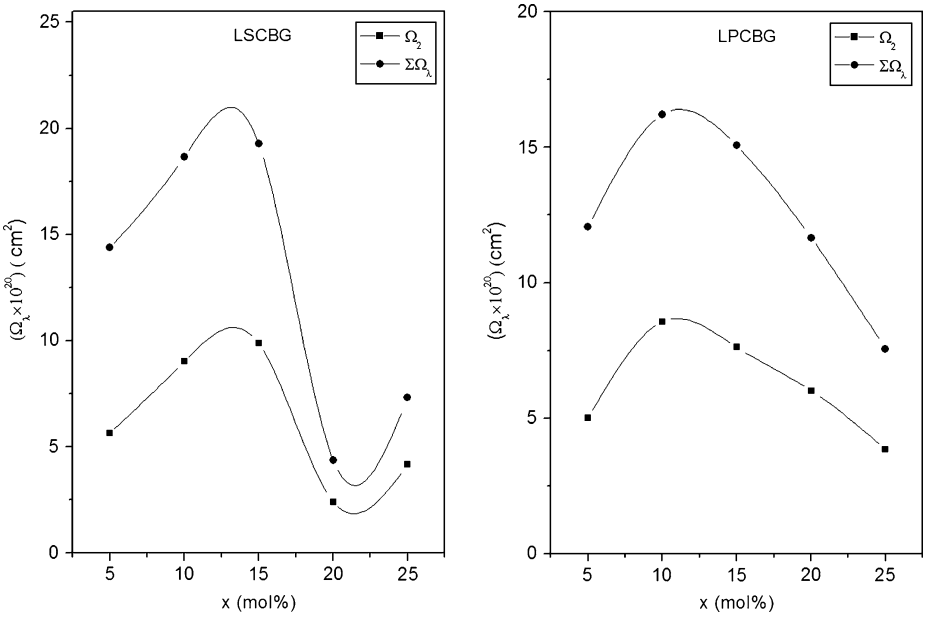

Fig. 2 Dependence of Ω_2 (covalency parameter) and $\Sigma\Omega_\lambda$ (sum of the Judd–Ofelt parameter) parameter on x (concentration of lithium content) in the two indicate mixed alkali chloro-botare glasses. Figure shows increasing and decreasing covalencies at higher lithium content (i.e., x=25 mol%) for lithium–sodium and lithium–potassium glass matrices, respectively

Judd [23] suggested that the spectral profile of the hypersensitive transition is strongly affected by changes in the symmetry of the crystal field acting on the rare earth ion. A difference in the shape of the absorption peak indicates a difference in the environment of Ho^{3+} ion. In the present work, the spectral profiles of the hypersensitive transition for different x values in both the glass matrices are slightly changing indicating the small changes in crystal field symmetry. The shift in peak wavelength of the HST towards longer wavelengths with an increase of alkali content is due to nephelauxtic effect [24], indicating that the degree of covalency of RE–O bond increases with the increase of alkali content. In the present work, in lithium–sodium glass, the covalency of Ho–O bond decreases with the increase of lithium content from 10 to 15 mol% as indicated by the shift of the hypersensitive band towards shorter wavelength. But the Ω_2 parameter increased at this composition. It can be observed from Eq. 3 that $A_{s,p}$ is responsible for the increase in Ω_2 parameter at this composition indicating some structural changes. Similarly at x=20–25 mol%, there is a small shift in HST towards shorter wavelength indicating decrease in covalency, but the Ω_2 parameter increases indicating that $A_{s,p}$ is responsible for this increase indicating small structural changes. In the case of lithium–potassium glass, at x=15–20 mol%, there is a shift of HST towards longer wavelength indicating increase in covalency, but the Ω_2 parameter decreases indicating changes in the crystal field symmetry around Ho^{3+} ion. Similarly at x=20–25 mol%, there is a small shift of HST towards longer wavelength, but the Ω_2 parameter decreases indicating small structural changes. These structural changes might be due to the "borate anomaly" that was explained in the introduction part.

From the above studies, it is observed that at x=5–10 mol%, in both lithium–sodium and lithium–potassium mixed alkali glass matrices, the changes in the symmetry of the crystal field around Ho^{3+} ions are the same. These changes are not influencing the covalency of Ho–O bond. At x=10–15 and 20–25 mol% of lithium–sodium glass, $A_{s,p}$ which indicates symmetry of the crystal field around Ho^{3+} is responsible for the increase or decrease in covalency. In lithium–potassium glass matrix also, at x=15–20 and 20–25 mol%, $A_{s,p}$ is responsible for the increase or decrease in covalency indicating changes in crystal field symmetry at these compositions.

3.3 Radiative Properties

Using Ω_λ, radiative transition probabilities (A_{rad}) of different transitions of Ho^{3+} were calculated in all the glass matrices with the relation [25]

$$A_{\mathrm{rad}}(aJ, bJ') = \frac{64\pi^4 e^2}{3h(2J+1)} \frac{1}{\lambda^3} \left[\frac{n(n^2+2)^2}{9} S_{\mathrm{ed}} + n^3 S_{\mathrm{md}} \right] \tag{4}$$

where S_{ed} and S_{md} denote the electric and magnetic dipole line strengths. The remaining symbols have their usual meanings. The total radiative transition probabilities, $A_T(=\sum A_{rad})$, radiative lifetimes, $\tau_R\left(=\left(\sum A_{rad}(aJ, bJ')\right)^{-1}\right)$, luminescent branching ratios, $\beta(=A_{rad}(aJ, bJ')/A_T(aJ'))$and integrated absorption cross-sections, $\sum\left(=\frac{1}{\nu^2}\times\frac{A}{8\pi cn^2}\right)$are determined for different excited levels. The estimated radiative lifetimes

(τ_R) of the excited states, $^3H_5$, $^5G_6$, $^3K_8$, $^5F_2$, $^5F_3$, $^5F_4$, and $^5F_5$ of Ho^{3+} ion in these two mixed alkali glass matrices are shown in Table 4. The error in estimated τ_R is ±5% for all the excited states. It is observed that the radiative lifetimes are higher and lower for $^3K_8$ and $^5G_6$ states respectively among various excited states in the two glass matrices. From the table, it is also observed that for most of the excited states, the radiative lifetimes are higher at x=20 mol% in lithium–sodium and at x=25 mol% in lithium–potassium chloroborate glasses. The radiative lifetimes are lower at x=10–15 mol% in both the glass matrices. The variation in τ_R values with the variation of x in the two glass matrices is shown in Fig. 3. The branching ratios (β) and integrated absorption cross-sections (∑) of certain transitions which have higher in magnitudes in these two glass matrices are presented in Table 5. From the table, it is observed that the transitions $^5G_6 \rightarrow {}^5I_8$ and $^3K_8 \rightarrow {}^5I_8$ have higher values of branching ratios among all the transitions. The branching ratio values for $^5G_6 \rightarrow {}^5I_8$ transition are in range 0.861–0.874 and 0.864–0.868 for LSCBG and LPCBG matrices respectively for different x values in the glass matrices. For $^3K_8 \rightarrow {}^5I_8$ transition, these values are in the range 0.880–0.885 for both the glass matrices. The integrated absorption cross-sections are higher for most of the transitions at x=10–15 mol% in these two glass matrices.

3.4 Nonradiative Properties

The exponential dependence of the multiphonon relaxation rate (W_{MPR}) on the energy gap to the next lower level, ΔE has been experimentally established for a number of crystals and glasses and is given by [26]

$$W_{MPR} = C \exp[-\alpha \Delta E](n(\omega, T) + 1)^P \quad (5)$$

where C and α are positive, host dependent constants, which are almost independent of the specific 4f level of trivalent rare earth ions except in a few cases, $n = 1/(\exp(\omega\hbar/KT) - 1)$ and $P = \Delta E/\hbar\omega(\hbar\omega = 1,400\,cm^{-1})$ (for borate glass) and KT=209 cm^{-1}. Using the above equation, nonradiative relaxation rate constants for various Ho^{3+} excited states in these two mixed alkali chloroborate glasses are calculated using the values $\alpha = 3.8\times10^{-3}$ cm and $C = 2.9\times10^{12}$ s^{-1} reported for borate glasses [27]. These values for x=5, 15, and 25 mol% in both the glass matrices are given below (for the other x values, the nonradiative transition rates are in the same range).

Excited state	LSCBG			LPCBG		
	x=5	x=15	x=25	x=5	x=15	x=25
$^5G_5$	4.38×10^9	2.58×10^9	3.10×10^9	5.27×10^9	2.60×10^9	2.39×10^9
$^5G_6$	1.46×10^{11}	1.35×10^{11}	1.10×10^{11}	1.25×10^{11}	1.27×10^{11}	1.36×10^{11}
$^3K_8$	6.62×10^{11}	7.73×10^{11}	8.60×10^{11}	6.39×10^{11}	7.61×10^{11}	8.44×10^{11}
$^5F_2$	6.79×10^{11}	6.25×10^{11}	6.90×10^{11}	6.06×10^{11}	6.90×10^{11}	7.36×10^{11}
$^5F_3$	1.19×10^9	1.25×10^9	1.18×10^9	1.23×10^9	1.18×10^9	1.10×10^9
$^5F_4$	1.23×10^{12}	1.30×10^{12}	1.23×10^{12}	1.25×10^{12}	1.23×10^{12}	1.23×10^{12}
$^5S_2$	6.80×10^7	6.55×10^7	6.80×10^7	6.83×10^7	7.65×10^7	6.99×10^7
$^5F_5$	2.23×10^5	2.27×10^5	2.06×10^5	2.19×10^5	1.99×10^5	2.29×10^5

Table 4 Radiative lifetimes (τ_R) (μs) of certain excited states of Ho^{3+} doped mixed alkali chloroborate glasses (x in mol%)

S.No	Glass matrix	$^3H_5$	$^5G_6$	$^3K_8$	$^5F_2$	$^5F_3$	$^5F_4$	$^5F_5$
	LSCBG							
1	x=5	34	24	909	173	125	115	188
2	x=10	25	18	668	131	101	97	163
3	x=15	26	19	609	117	97	99	178
4	x=20	108	79	2,517	482	403	419	760
5	x=25	64	46	1,582	314	256	265	474
	LPCBG							
6	x=5	40	28	1,178	232	165	148	237
7	x=10	29	21	726	143	114	114	200
8	x=15	31	23	742	143	114	116	203
9	x=20	41	30	899	168	140	145	262
10	x=25	63	47	1,398	263	215	223	402

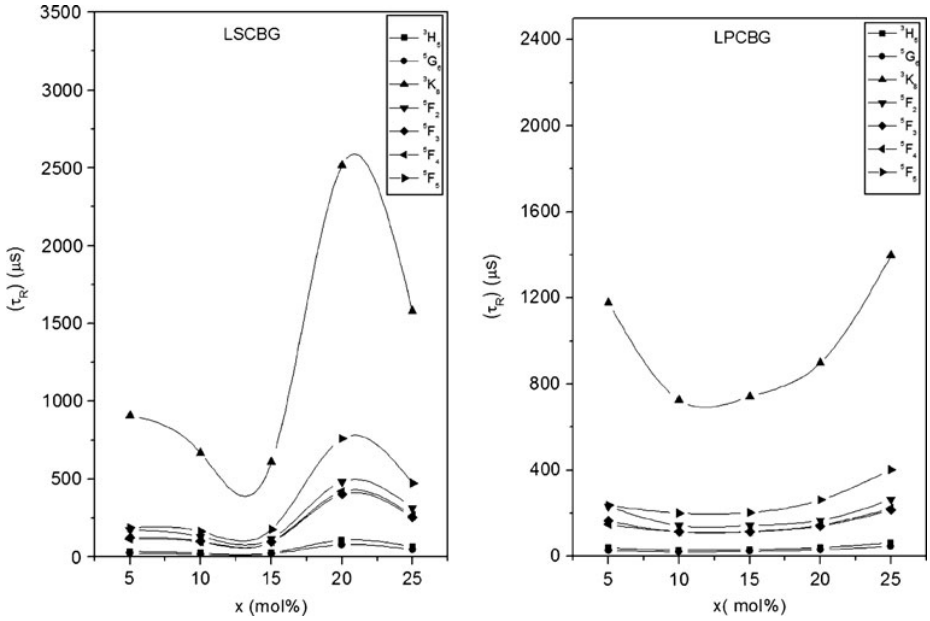

Fig. 3 Dependence of radiative lifetime, τ_R on x (concentration of lithium content) in two indicate mixed alkali chloro-borate glass matrices. Figure shows decreasing and increasing lifetime at x=25% (at higher lithium content) in lithium–sodium and lithium–potassium glass matrices, respectively

It is observed that the nonradiative relaxation rates are higher for $^5F_4$ level and lower for $^5F_5$ level among various excited levels. It is also observed that the nonradiative relaxation rates are increased at x=15 mol% in the case of $^5F_5$ level. In the case of $^5F_4$ level, nonradiative relaxation rates are increased at x=15 mol% in LSCBG glass and decreased in LPCBG glass.

3.5 Emission Properties

Good laser transitions are characterized by large cross-section for stimulated emission. In the present work, the stimulated emission cross-sections (σ_p) are obtained from the spectroscopic data using the formula [28]

$$\sigma_P = \frac{\lambda_P^4}{8\pi c n^2 \Delta\lambda_{eff}} A_{rad}(aJ, bJ) \tag{6}$$

where, n is the refractive index of the host material, C is the velocity of light, A_{rad} is the radiative transition probability, λ_p is the peak wavelength and $\Delta\lambda_{eff}$ is effective line width. The effective line width $\Delta\lambda_{eff}$ of the emission band is obtained from

$$\Delta\lambda_{eff} = \frac{\int I(\lambda)}{I_{max}} d\lambda \tag{7}$$

Table 5 Branching ratios (β) and integrated absorption cross-sections ($\sum\times10^{-18}$ cm^{-1}) of certain transitions of Ho^{3+} doped mixed alkali chloroborate glasses (x in mol%)

S. no	Glass matrix	$^3H_5\rightarrow{}^5I_7$		$^5G_6\rightarrow{}^5I_8$		$^3K_8\rightarrow{}^5I_8$		$^5F_2\rightarrow{}^5I_8$		$^5F_3\rightarrow{}^5I_7$		$^5F_4\rightarrow{}^5I_8$		$^5F_5\rightarrow{}^5I_8$	
		β	∑	β	∑	β	∑	β	∑	β	∑	β	∑	β	∑
	LSCBG														
1	x=5	0.591	16.1	0.844	34.7	0.884	1.1	0.406	2.5	0.453	6.9	0.730	8.95	0.748	8.04
2	x=10	0.641	23.3	0.861	47.0	0.881	1.6	0.467	3.8	0.399	7.6	0.758	11.38	0.742	9.17
3	x=15	0.670	24.0	0.870	46.9	0.883	1.5	0.535	4.9	0.330	6.5	0.799	11.06	0.735	8.35
4	x=20	0.676	5.8	0.871	11.0	0.880	0.4	0.546	1.2	0.318	1.5	0.806	2.73	0.734	1.96
5	x=25	0.686	9.9	0.874	18.9	0.881	0.6	0.537	1.8	0.329	2.4	0.799	4.29	0.734	3.14
	LPCBG														
6	x=5	0.605	14.0	0.848	30.1	0.885	0.8	0.337	3.8	0.481	5.6	0.717	6.87	0.749	6.42
7	x=10	0.665	21.1	0.868	41.1	0.881	1.4	0.221	4.2	0.354	5.9	0.783	9.73	0.737	7.46
8	x=15	0.652	19.0	0.864	37.3	0.881	1.3	0.216	4.2	0.347	5.8	0.788	9.66	0.737	7.32
9	x=20	0.656	14.8	0.865	28.5	0.880	1.1	0.197	3.2	0.320	4.4	0.805	7.86	0.735	5.66
10	x=25	0.653	9.5	0.864	18.4	0.880	0.7	0.201	2.1	0.326	2.9	0.802	5.09	0.736	3.71

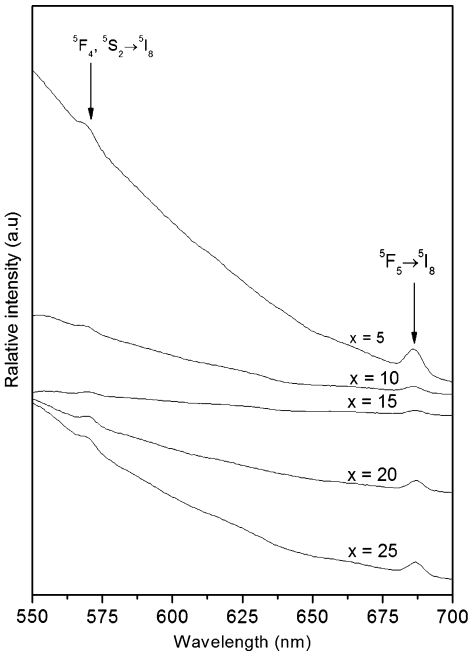

Fig. 4 Emission spectra of Ho^{3+} doped lithium–sodium mixed alkali chloroborate glasses at room temperature: the excitation wavelength is 418 nm

where I is the emission intensity and I_{max} is the intensity at band maximum.

The emission spectra of Ho^{3+} doped lithium–sodium mixed alkali chloroborate glass for different x values in the glass matrix in the wavelength range 500–700 nm, with line of excitation, 418 nm are shown in Fig. 4. The emission spectra of Ho^{3+} ion in lithium–potassium mixed alkali chloroborate glass matrix are not shown, as they are similar in shape. In the present work, two emission bands are observed nearly at 570 nm (green) and 686 nm (red) and are assigned to the transitions, $^5F_4$, $^5S_2 \rightarrow {}^5I_8$ and $^5F_5 \rightarrow {}^5I_8$ [29, 30] respectively. Using Eq. 6, emission cross-sections were calculated for these two emission transitions in these two glass matrices and are presented in Table 6. It is observed that between the two transitions, the transition $^5F_4$, $^5S_2 \rightarrow {}^5I_8$ has higher emission cross-section at x= 10 mol% in both the glass matrices. On the basis of these studies, it is concluded that among all the mixed alkali chloroborate glasses studied, the glasses with x=10 mol% may be useful for laser excitation as the transition $^5F_4$, $^5S_2 \rightarrow {}^5I_8$ has higher emission cross-section.

4 Conclusions

The nonsymmetric component of crystal field acting on Ho^{3+} ions is stronger and weaker at x=10–15 mol% and at x=20–25 mol% respectively in both lithium–sodium and lithium–potassium mixed alkali chloroborate glasses. Among different x values in the glass matrices, Ω_2 parameter is larger at x=15 mol% in lithium–sodium and at x=10 mol% in lithium–potassium mixed alkali glasses indicating higher covalency at these compositions. From the variation of shift in the position of peak wavelength of the hypersensitive transition and Ω_2 parameter with the variation of x in the glass matrices, it is concluded that at x=10–15 and 20–25 mol% in lithium–sodium glass, and at x=15–20 and 20–25 mol% in lithium–potassium glass, changes in the symmetry of the crystal field around Ho^{3+} is responsible for the increase/decrease in covalency of Ho–O bond indicating structural changes. The radiative lifetimes are higher for $^3K_8$ state and lower for $^5G_6$ state among various excited states in the two glass matrices. For

Table 6 Certain emission properties of Ho^{3+} doped mixed alkali chloroborate glasses (x in mol%)

S. no	Glass matrix	$^5F_4$, $^5S_2 \rightarrow {}^5I_8$				$^5F_5 \rightarrow {}^5I_8$			
		λ_p (nm)	A_{rad} (s^{-1})	$\Delta\upsilon_{eff}$ (cm^{-1})	$\sigma_p \times 10^{-20}$ (cm^2)	λ_p (nm)	A_{rad} (s^{-1})	$\Delta\upsilon_{eff}$ (cm^{-1})	$\sigma_p \times 10^{-20}$ cm^2
	LSCBG								
1	x=5	567	6,307	229	4.37	686	3,971	215	4.28
2	x=10	568	7,806	202	6.12	686	4,545	227	4.64
3	x=15	570	8,017	425	3.00	685	4,125	202	4.71
4	x=20	570	1,923	188	1.64	687	965	165	1.36
5	x=25	569	3,015	155	3.09	687	1,547	198	1.82
	LPCBG								
6	x=5	570	4,827	326	2.36	688	3,161	204	3.60
7	x=10	570	6,850	150	7.33	688	3,682	175	4.88
8	x=15	568	6,803	243	.4.45	685	3,629	237	3.54
9	x=20	569	5,536	256	3.54	686	2,805	179	3.43
10	x=25	569	3,585	179	3.20	686	1,831	220	1.93

most of the excited states, the radiative lifetimes are higher at x=20 mol% in lithium–sodium and at x=25 mol% in lithium–potassium chloroborate glasses. Between the two emission transitions observed in the present work, $^5F_4$, $^5S_2 \rightarrow {}^5I_8$ transition has higher emission cross-section at x=10 mol% in both the glass matrices. On the basis of these studies, it is concluded that among all the mixed alkali chloroborate glasses studied, the glasses with x= 10 mol% may be useful for laser excitation.

Acknowledgements The author YCR expresses his thanks to the University Grants Commission, New Delhi for providing the financial assistance in the form of major research project.

References

1. S. Hazarika, S. Rai, Opt. Mater ., **27**, 173 (2004).
2. J.H. Campbell, T. I. Suratwala, J. Non-Cryst. Solids **318**, 263 (2000).
3. R. Reisfeld, C.K. Jorgensen, Phys. Rev., **B13**, 81 (1976).
4. S.D. Jackson, IEEE, J. Quantum Electron, **42**, 187 (2006).
5. S.D. Jackson, S. Mossman, Appl. Opt., **42,(18)** 3546 (2003).
6. D.W. Hart, M. Jani, N.P. Barnes, Opt. Lett. **21**, 728 (1996).
7. A.A. Kaminskii, T.I. Butaeva,A.O. Ivanov, T.V. Mochalov, A.G. Petrosyan, G.I. Rogov, V.A. Fedorov, Sov. Tech. Phys. Lett. **2**, 308 (1976).
8. A.A. Kaminskii, V.A. Fedorov, S.E. Sarkisov, J. Bohm, P. Reiche, D. Scultze, Phys. Stat. Sol. (a) **53,** 219 (1979).
9. P.R. Watekar, Seongmin Ju, Won-Taek Han, J. Non-Cryst. Solids **354**, 1453 (2008).
10. Tae Hoon Lee, Ypung Kon Kwon, Jong Heo, J. Non-Cryst. Solids **354**, 3107 (2008).
11. M. Seshadri, Y.C. Ratnakaram, D. Tirupathi Naidu, K. Venkata Rao, J. Lumin. **130,** 536 (2010).
12. D. Piatkowski, K. Wisniewski, M. Rozanski, Cz. Koepke, M. Kaczken, M. Klinczak, R. Plimczak, R. Piramidowicz, M. Malinowski, J. Phys.: Condens. Matter **20**, 155201 (11 pp) (2008).
13. Li Feng, Jing Wang, Qiang Tang, Lifang Liang,, Hongbin Lianga, Qiang Su, J. Lumin. **124**, 187 (2007).
14. D.E. Day, J. Non-Cryst. Solids, 21, 343 (1976).
15. J. Bisco and B.E. Warren, J. Am. Ceram. Soc., 21, 287 (1938)
16. H. Rawson, Inorganic glass forming systems, Academic Press, London (1967).
17. W.T. Carnall and H. Crosswhite and H.M. Crosswhite "Energy level structure and transition probabilities in the spectra of trivalent lanthanides in LaF_3". Argonne National Laboratory Report (1977).
18. E.Y. Wong, J. Chem. Phys., **35,** 544 (1961).
19. B.R. Judd, Phys. Rev., **127**, 750 (1962).
20. G.S. Ofelt, J. Chem. Phys., **37**, 511 (1962).
21. R.D. Peacock, Structure and bonding, Springer, NewYork (Berlin), 22 (1975).
22. R. Reisfeld, Structure and bonding, Springer, Berlin, **22**, (1975).
23. B.R. Judd, Proc. Phys. Sco. London, Ser. A **69,** 157 (1956).
24. C.K. Jorgensen, Prog. Inorg. Chem. **4**, 73 (1962).
25. Y.C. Ratnakaram, R.P.S. Chakradhar, K.P. Ramesh, J.L. Rao and J. Ramakrishna J. Mater. Sci., **38**, 833 (2003).
26. M. Shojiya, Y. Kawamoto and K. Kadono, J. Appl. Phys. **89,** 4944 (2001).
27. M. Shojiya, M. Takahashi, R. Kanno et al., ibid, 82.
28. M. Yamene and Y. Asahara, Glasses for photonics, Cambridge University Press, Cambridge (2000).
29. J.C. Boyer, F. Vetrone, J.A. Capobianco, A. Speghini, J. Appl. Phys., **93**, 9460 (2003).
30. G.A. Kumar, A. Martinex, E. Mejia, J.G. Eden, J. Alloys Compd. **365**, 4117 (2004).